



**HAL**  
open science

# Nucleophilic or Electrophilic Interactions of C2 with HX systems (X=F, Cl, Br)

D. Khiri, H. Gritli, Gilberte Chambaud

► **To cite this version:**

D. Khiri, H. Gritli, Gilberte Chambaud. Nucleophilic or Electrophilic Interactions of C2 with HX systems (X=F, Cl, Br). *Journal of Physical Chemistry A*, 2014, 118 (32), pp.6248. 10.1021/jp503651u . hal-01064801

**HAL Id: hal-01064801**

**<https://hal.science/hal-01064801>**

Submitted on 17 Sep 2014

**HAL** is a multi-disciplinary open access archive for the deposit and dissemination of scientific research documents, whether they are published or not. The documents may come from teaching and research institutions in France or abroad, or from public or private research centers.

L'archive ouverte pluridisciplinaire **HAL**, est destinée au dépôt et à la diffusion de documents scientifiques de niveau recherche, publiés ou non, émanant des établissements d'enseignement et de recherche français ou étrangers, des laboratoires publics ou privés.

# Nucleophilic or Electrophilic Interactions of C<sub>2</sub> with HX Systems (X = F, Cl, Br)

D. Khiri,<sup>†,‡</sup> H. Gritli,<sup>†</sup> and G. Chambaud<sup>\*,‡</sup>

*Université de Tunis, Laboratoire de Spectroscopie Atomique Moléculaire et Applications  
LSAMA, Tunis, Tunisia, and Université Paris-Est Marne-la-Vallée, Laboratoire MSME,  
UMR-8208 CNRS, Cité Descartes, Champs-sur-Marne, 77454, Marne-la-Vallée, France*

E-mail: gilberte.chambaud@u-pem.fr

---

\*To whom correspondence should be addressed

<sup>†</sup>Université de Tunis, Laboratoire de Spectroscopie Atomique Moléculaire et Applications LSAMA, Tunis, Tunisia

<sup>‡</sup>Université Paris-Est Marne-la-Vallée, Laboratoire MSME, UMR-8208 CNRS, Cité Descartes, Champs-sur-Marne, 77454, Marne-la-Vallée, France

## Abstract

Highly correlated *ab-initio* wavefunctions within the MRCI approach are used in a comparative study of the interactions between  $C_2$  and the three hydrogen halides HX ( $X = F, Cl, Br$ ). Test calculations are also presented using the UCCSD(T)-F12 approach. The asymptotic regions are investigated for different relative orientations of the two moieties. It is shown that the three systems  $C_2 + HX$  are bound, for intermolecular distances close to 3 Å, through nucleophilic interactions between  $C_2$  and HX for approaches perpendicular to the C-C axis, with decreasing interaction energies from HF to HBr. For HX approaching  $C_2$  along its axis, the interactions, governed by the electrophilic character of  $C_2$  are decreasing from HBr to HF. Even though the reactions towards the molecular systems HCCX or CCHX are exothermic, activation barriers (0.58 eV and more) are calculated at short distances, preventing the direct reactions towards the corresponding tetra-atomic systems.

Keywords : Potential curves, long range interactions, ab-initio calculations, hydrogen halides

## Introduction

Small carbon clusters and particularly  $C_2$  have been subject of numerous studies for their interest in the understanding of the chemistry of the interstellar medium, the cometary tails and cool carbon stars.  $C_2$  is also found in flames and electric discharges through materials containing carbon. Structural properties and spectroscopy of  $C_2$  have been widely investigated theoretically (see for exemple <sup>1-9</sup>) and also experimentally.<sup>10,11</sup> Many reactions involving  $C_2$  are known, among them the reaction or interactions with  $H^{12}$  or  $H_2$ ,<sup>13-15</sup> however only few is known about the reaction paths or about the stability against dissociation of the reaction products. In this paper, we investigate the interactions at low energy between  $C_2$  and HX and examine the possibility of a direct reaction that could lead to the molecular system  $C_2HX$  either in the linear stable form XCCH of  $C_{\infty v}$  symmetry or in the planar iso form  $C_2HX$  of  $C_s$  symmetry. Such study could be of interest for the chemistry of atmosphere or interstellar medium where  $C_2$  is ubiquitous.

The long range interactions between  $C_2$  and the polarised HX molecules are governed by several combined effects: dipole-quadrupole interactions, dispersion, orbital overlapping and charge transfers. They can also be described in terms of the nucleophilic or electrophilic character of  $C_2$  depending on the relative orientation of the reactants. The electronic structure and the reactivity of the low lying states of  $C_2$  can be essentially discussed by considering the occupancy of the two following valence molecular orbitals: the bonding  $1\pi_u$  and the quasi non-bonding  $3\sigma_g$ . In the ( $X^1\Sigma_g^+$ ) ground state the major configuration is ( $\dots, 2\sigma_g^2, 2\sigma_u^2, 1\pi_u^4$ ) and in the first excited state ( $a^3\Pi_u$ ), it is ( $\dots, 2\sigma_g^2, 2\sigma_u^2, 1\pi_u^3, 3\sigma_g^1$ ). Due to its full  $1\pi_u$  orbital, the  $C_2$  molecule exhibits a large electronic density around the C-C axis providing a nucleophilic character towards reactants approaching  $C_2$  perpendicularly to its axis: the ( $X^1\Sigma_g^+$ ) or the ( $a^3\Pi_u$ ) states (in that case, more specifically one of the  $\Pi$  component) present this characteristic. For electronic configurations where the  $3\sigma_g$  orbital is empty, namely for the ( $X^1\Sigma_g^+$ ) ground state,  $C_2$  can also show electrophilic character towards reactants approaching along the C-C axis and bringing electrons by charge transfer into this  $3\sigma_g$  orbital. In both cases, relatively strong interactions can occur. Moreover, since the two orbitals ( $1\pi_u$  and  $3\sigma_g$ ) are energetically close, the first two electronic states are only separated by  $716\text{ cm}^{-1}$ .<sup>10,11</sup> It is thus necessary to investigate the reactivity of  $C_2$  in both singlet and triplet spin symmetries: here the singlet [ $C_2(X^1\Sigma_g^+) + HX(X^1\Sigma^+)$ ] and the triplet [ $C_2(a^3\Pi_u) + HX(X^1\Sigma^+)$ ] channels have been studied for parallel, collinear and several perpendicular approaches.

In fact, the situation cannot be described so simply because of the multi-configurational character of the ( $X^1\Sigma_g^+$ ) ground state: the coefficient of its dominant valence configuration ( $\dots, 2\sigma_g^2, 2\sigma_u^2, 1\pi_u^4$ ) is only 0.83 in the CASSCF or MRCI wavefunction expansion<sup>1,3,5,6</sup> completed by the doubly excited configuration ( $\dots, 2\sigma_g^2, 1\pi_u^4, 3\sigma_g^2$ ) with a rather large coefficient of 0.33. For the ( $a^3\Pi_u$ ) state there is no such intra valence correlation and the coefficient of the dominant configuration is always close to 0.94. As a consequence of the multi-configurational character of the ( $X^1\Sigma_g^+$ ) state of  $C_2$ , the usual single reference methods have to be considered carefully as already pointed out in the benchmark calculations of Watts and Bartlett.<sup>1</sup> For this reason we privileged here the MRCI approach but we compared some results with those obtained via explicitly correlated UCCSD(T)-F12

calculations.<sup>17,18</sup>

## Electronic calculation details

All electronic structure calculations have been performed with the MOLPRO program package,<sup>16</sup> using the MRCI and UCCSD(T)-F12 methods to calculate the energies and some properties of the electronic states. In the MRCI calculations, the molecular orbitals have been optimized in a preceding full-valence CASSCF step. In order to limit the size of the resulting CI matrices, only configurations with a coefficient larger than 0.001 in the CASSCF wavefunction expansion were included in the reference set for each geometry, yielding a dimension of approximately  $3 \times 10^9$  configurations for the MRCI matrix. The Davidson correction has been applied, leading to deeper minima in the Potential Energy Surfaces (PES) without changing the general trends of the results. The basis set superposition error (BSSE) has been corrected at all geometries of the long range interactions in the  $C_2 + HX$  systems according to the Boys and Bernardi counterpoise scheme.<sup>19</sup> Even though the MRCI methods are not size-consistent, such an ansatz should provide reliable data. In order to validate such a procedure, two different types of basis sets have been used: the aug-cc-pVTZ basis sets of Dunning<sup>20</sup> (or equivalent) to compare the MRCI and the UCCSD(T)-F12 calculations, because it has been recently shown<sup>21</sup> that this type of basis set provides accurate results for the UCCSD(T)-F12 method, and the aug-cc-pVQZ basis sets of Dunning<sup>20</sup> which certainly lead to more accurate results for long range interactions at the MRCI level.

For the halogen atoms, we used the core pseudo-potentials ECPnMWB,<sup>22</sup> with  $n = 2, 10, 28$  for F, Cl and Br respectively in order to treat the same number of effective electrons for the three systems. For the carbon and hydrogen atoms, the two different types of Dunning basis sets have been used.

For the fluorine atom, we used the ECP2MWB<sup>22</sup> basis set including (4s,5p)/(2s,3p) functions augmented by 2 additional s type functions (exponents : 0.12, 0.035), 1 p function (exponent : 0.021), 3 d functions (exponents : 3.10, 0.85, 0.29) and 2 f functions (exponents : 1.91, 0.72),

resulting in a (6s, 6p, 3d, 2f) / (4s, 4p, 3d, 2f) set, equivalent to an aug-cc-pVTZ basis. We used also the Dunning aug-cc-pVQZ basis set (13s, 7p, 4d, 3f, 2g) / (6s, 5p, 4d, 3f, 2g).

Similarly, for the chlorine atom, we used, equivalent to an aug-cc-pVTZ basis, the ECP10MWB<sup>22</sup> basis set including (4s,5p)/(2s,3p) functions augmented by 2 additional s type functions (exponents : 0.065, 0.025), 1 p function (exponent : 0.005), 3 d functions (exponents : 1.046, 0.34, 0.13) and 2 f functions (exponents : 0.70, 0.31), resulting in a (6s, 6p, 3d, 2f) / (4s, 4p, 3d, 2f) set, and we also used the Dunning aug-cc-pVQZ basis set (17s,12p, 4d, 3f, 2g)/(7s, 6p, 4d, 3f, 2g).

For the bromine atom, we used the ECP28MWB-AVTZ<sup>23</sup> basis set corresponding to (15s, 11p, 3d, 2f) / (4s, 4p, 3d, 2f) and the ECP28MWB-AVQZ<sup>23</sup> basis set corresponding to (15s, 11p, 4d, 3f, 2g) / (5s, 5p, 4d, 3f, 2g).

In the following we used the shorthand notation aVQZ and aVTZ for the two types of basis sets.

## Structural and energetic data on the diatomic fragments

The electronic energies and some properties of the atoms and of the diatomic fragments involved in this study are reported in Table 1 and compared with previous calculations and/or available experimental data. The equilibrium bond lengths  $R_e$  and the harmonic frequencies  $\omega_e$  of the two electronic states of  $C_2$  are calculated very close to the experimental values. The experimental splitting,  $T_e$ ,<sup>24</sup> between these two electronic states ( $\Delta E_{exp} = 716 \text{ cm}^{-1}$ ) is satisfactorily reproduced in our MRCI calculations ( $\Delta E = 877 \text{ cm}^{-1}$  and  $687^* \text{ cm}^{-1}$  for the aVQZ and aVTZ basis set respectively), and also in the UCCSD(T)-F12 calculations with the aVTZ basis set ( $\Delta E_{UCCSD(T)-F12a} = 908 \text{ cm}^{-1}$ ,  $\Delta E_{UCCSD(T)-F12b} = 741 \text{ cm}^{-1}$ ). The MRCI calculated polarisability of  $C_2$  is also very close to previous calculated value using MRCI method<sup>14</sup> but significantly different from the overestimated values of  $\alpha_{iso} = 35.9 \text{ a.u.}$  obtained with the UCCSD(T)-F12a calculation. The average polarisabilities  $\alpha_{iso}$  given in Table 1 are defined as  $3\alpha_{iso} = 2\alpha_{perp} + \alpha_{para}$ .

The equilibrium bond lengths  $R_e$  and the harmonic frequencies  $\omega_e$  of the diatomics HX are also calculated very close to the experimental values. As for  $C_2$ , these quantities are deduced from a

treatment with the Numerov algorithm of the potential energy curve of the diatomics calculated for distances between 0.8 and 4 Å. The calculated dissociation energies of HX (with the aVQZ basis set for MRCI and the aVTZ one for UCCSD(T)) are in good agreement with the experimental values: for HF,  $D_{0[MRCI]} = 5.775$  eV,  $D_{0[UCCSD(T)-F12a]} = 5.706$  eV and  $D_{0[UCCSD(T)-F12b]} = 5.684$  eV to be compared with  $D_{0exp} = 5.869$  eV, for HCl,  $D_{0[MRCI]} = 4.415$  eV,  $D_{0[UCCSD(T)-F12a]} = 4.474$  eV and  $D_{0[UCCSD(T)-F12b]} = 4.465$  eV when  $D_{0exp} = 4.434$  eV and for HBr,  $D_{0[MRCI]} = 3.803$  eV,  $D_{0[UCCSD(T)-F12a]} = 3.915$  eV and  $D_{0[UCCSD(T)-F12b]} = 3.906$  eV and  $D_{0exp} = 3.758$  eV. The dipole moments at equilibrium bond length of the hydrogen halides and their average polarisabilities, with both basis sets, also show good agreement with experimental and previous calculated values. For the chlorine system, the so-called aVTZ basis set has been designed for the pseudo-potential of chlorine and it gives satisfactory results for the HCl molecule, however for the long range interactions it is not sufficient and leads to too large BSSE corrections (see Supplementary Materials). A good agreement obtained on these quantities was a necessary requirement to propose reliable data in the subsequent comparative study on this family of systems.

The equilibrium bond lengths of the linear HCCX and the iso C<sub>2</sub>HX and their energies relative to their respective dissociation limits, calculated at the MRCI level of theory with the two different basis sets, are given in Table 2. The reactions C<sub>2</sub> + HX leading to the two isomeric forms are found exothermic for the three hydrogen halides. The linear forms are significantly more stable energetically than the iso forms (by more than 2 eV) and they are separated by a very small barrier (a fraction of eV larger than these energy differences). The C-C bond in the linear HCCX is shorter than in C<sub>2</sub>(X<sup>1</sup>Σ<sub>g</sub><sup>+</sup>) showing that the triple bond character of C-C has been reinforced by creating the two new bonds involving the participation of the anti-bonding 2σ<sub>u</sub> orbital. On contrary, the C-C bond in the iso CCHX form is longer than in C<sub>2</sub>(X<sup>1</sup>Σ<sub>g</sub><sup>+</sup>) showing the participation of the 1π<sub>u</sub> electrons in the formation of the two new bonds. This table shows that, at the equilibrium geometry determined at the MRCI level, the relative energies calculated with the two different basis are very close for the chlorine and bromine compounds. Similar calculations with the UCCSD(T)-F12 method give relative energies different by less than 0.2 eV from the MRCI ones. On contrary, for

the fluorine halide, the MRCI relative energies of both isomers are much smaller with the aVQZ basis set than with the aVTZ one: the relative energies calculated with the UCCSD(T)-F12 method and the aVTZ basis set are -2.793 eV and -4.752 eV, for the iso and linear forms respectively showing that, for such mono-configurational systems, the UCCSD(T)-F12 associated with aVTZ basis set can be as efficient as MRCI method with a larger basis set.

Considering the above results on the two moieties, the best strategy to describe the interactions between  $C_2$  and HX consists in using multi-configurational methods (MRCI + corrections) and large enough basis sets (aVQZ quality).

## Potential Energy Surfaces

In order to map the largest part of the Potential Energy Surfaces, PES, for long and intermediate intermolecular distances of the tetra-atomic systems correlated with the first two dissociation limits, the singlet [ $C_2(X^1\Sigma_g^+) + HX(X^1\Sigma^+)$ ] and the triplet [ $C_2(a^3\Pi_u) + HX(X^1\Sigma^+)$ ], a set of different approaches of the two fragments  $C_2$  and HX has been selected : the relative orientations are represented and labelled on Figure 1. The two moieties are kept either collinear or in the same plane, except for the cross orientation where HX approaches perpendicularly the C-C bond in a perpendicular plane. In the molecular region, the singlet [ $C_2(X^1\Sigma_g^+) + HX(X^1\Sigma^+)$ ] dissociation limit gives a  $X^1\Sigma^+$  state for collinear geometries and a  $^1A'$  state for all other selected geometries, the triplet [ $C_2(a^3\Pi_u) + HX(X^1\Sigma^+)$ ] gives a degenerate  $^3\Pi$  state at linearity and two components,  $^3A'$  and  $^3A''$  states for all other selected geometries. The bond lengths of the diatomics have been varied when approaching the two fragments: it is found that, except when the systems are approaching the barrier towards the tetra-atomic species, the diatomic fragments keep the equilibrium geometry of the isolated diatomics.

The cuts of the PESs (MRCI+Davidson correction+BSSE), calculated with the aVQZ basis set and plotted for fixed values of the diatomics bond lengths, are given in Figure 2 to Figure 7 for the three halogen systems and are functions of the distance  $d_e$  between the center of  $C_2$  and the

center of HX. These cuts show deep or shallow minima in singlet and in some triplet states for separations close to 3 Å. The main characteristics of these minima,  $d_e$  and the interaction energies  $\Delta E$  are given in Table 3 for the three halogen systems. It is found (see Supplementary Materials section) that the BSSE corrections are rather large when using the aVTZ basis set, but it is quite satisfactory to observe that the corrected values, including the BSSE correction, are rather close with the two basis sets.

For all systems and all relative orientations, there is a barrier at short  $d_e$ , before the decreasing of the energy towards either the linear HCCX or the iso C<sub>2</sub>HX isomers.

## Nature and strength of the interactions

For HX approaching perpendicularly to the C-C axis, the  $X^1\Sigma_g^+$  state of C<sub>2</sub> shows nucleophilic character due to its in-plane closed shell  $1\pi_u$  orbital. The same nucleophilic character is observed for the  $^3A''$  component of the  $^3\Pi_u$  state. On contrary, the  $^3A'$  component is slightly electrophilic due to the half-full in-plane  $1\pi_u$  orbital of C<sub>2</sub>. For HF and HCl systems, the overall largest interactions correspond to the perpendicular approach 1 with the hydrogen atom pointing towards the nucleophilic C<sub>2</sub>, as expected from the  $H^{+\delta}X^{-\delta}$  polarisation of the bond. For the three systems, the shapes of the potential cuts for the  $X^1A'$  and the  $^3A''$  states are very similar. The perpendicular interaction energies in the  $X^1A'$  state are larger for HX (1084 cm<sup>-1</sup>, 588 cm<sup>-1</sup> and 517 cm<sup>-1</sup>, for HF, HCl, HBr respectively at MRCI+Q+BSSE level) than for H<sub>2</sub> (101 cm<sup>-1</sup>)<sup>14</sup> due to the strong polarisation of the HX bond. For the second perpendicular orientation, when the halogen of HX is pointing towards the C-C bond, the interaction energies are smaller and mainly governed by the polarisabilities, explaining why the interaction energy is larger for HBr than for HCl and HF.

In the parallel approach the interaction energy, governed by the dispersion, is smaller than in the perpendicular one, resulting from smaller perpendicular polarisabilities than parallel ones for all the diatomics involved here. As in a previous study on the [C<sub>2</sub> + H<sub>2</sub>] system<sup>14</sup> it has been found that the cross approach presents a rather similar behaviour as the parallel one.

For the three orientations of HX approaching along the C-C axis, the interactions are governed by the dipole of HX, the polarisabilities of both HX and C<sub>2</sub> bonds and by the orbital effects. The 3σ<sub>g</sub> orbital of C<sub>2</sub> can play an important role in these interactions by accepting electrons by partial charge transfert from the HX molecule : this is the case for the X<sup>1</sup>A' state in T-shape approach when the π electrons of HX can be transferred to C<sub>2</sub> and, to a lesser extend in linear approach 2 when the X atom is pointing towards C<sub>2</sub> because the σ electrons of HX are less accessible than the π ones. This shows the electrophilic character of the X<sup>1</sup>Σ<sub>g</sub><sup>+</sup> state of C<sub>2</sub>. Because of these possible orbital overlaps or charge transferts, the multi-configurational character of the X<sup>1</sup>Σ<sub>g</sub><sup>+</sup> state of C<sub>2</sub> changes when HX approaches, leading to spurious effects in UCCSD(T)-F12 calculations.

In situations where this 3σ<sub>g</sub> orbital of C<sub>2</sub> contains one electron, namely the <sup>3</sup>Π state, a stabilizing electronic transfert towards the positively polarised hydrogen atom is possible, as observed on Figure 2, Figure 4 and Figure 6 for the linear approach 1. This evidences the weak nucleophilic character of this excited state of C<sub>2</sub>.

For the T-shape geometries, the values reported in Table 3 and the potential cuts for these approaches correspond to a position of the center of the HX bond exactly located on the C-C axis. For these T-shape orientations, additional calculations have been performed, in which the position of the center of HX has been moved up and down along the X axis with respect to the C-C axis. It has been found that the absolute minima (lower by 0.011 eV, 0.006 eV and 0.024 eV than for the position of the center of HX located on the C-C axis, for HF, HCl and HBr respectively) are obtained when the halogen atom is very close to the axis. The depths of these minima are increasing from HF to HBr due to the larger perpendicular polarisability of HBr than that of HCl and HF.

As in the C<sub>2</sub> + H<sub>2</sub> case, perpendicular and T-shape approaches are the most energetic ones.

The nature of the interaction between C<sub>2</sub> and HX is different in the two situations with the largest interactions, namely perpendicular approach 1 (nucleophilic) and T-shape (electrophilic). We have studied the variation of energy of the X<sup>1</sup>A' state between these two extreme situations by moving the HX molecule, kept parallel to the X axis, around C<sub>2</sub> by varying the angle α and the

distance  $d_e$  as described on Figure 8. The nature of the interaction changes for angle  $\sim 35$  deg for the three halogen systems (31 deg for HF, 35 for HCl and 36 for HBr) without any intermediate mixing of the two effects: there is no evidence of a specific stabilization energy for this transition situation between electrophilic (T-shape) and nucleophilic (perp 1) attraction effects. For all halogen systems, it is found that these long range PES are strongly anisotropic.

## Transition states to the tetra-atomics

At low energy the direct reactions towards the tetra-atomic systems are not possible but if enough energy is provided to the system, it can evolve towards the linear HCCX form or the iso form C<sub>2</sub>HX via transition states. For perpendicular and parallel approaches, the transition state  $TS(^1A')$  is found, at the MRCI level, as a stretched HX quasi parallel to C<sub>2</sub>. The creation of the C-H and C-X bonds is concerted with the breaking of the H-X bond, giving activation energies (energies necessary to reach the barrier) smaller by approximately 3-4 eV than the dissociation of the H-X bonds. The characterisation of these transition states is given in Table 4: the corresponding values are obtained through an automatic optimisation procedure involving about 100 iterations with steps of 0.01 Å, for each variable ( $d_e$ ,  $R_{HX}$ ,  $R_{CC}$ ), starting from a pre-searched position of the barrier. For approaches along the C-C axis, a secondary transition state  $TS'(^1A')$  is found, much higher than the first one (see Table 4). In this second transition state, the C-C bond slightly increases and the H-X bond starts also to stretch requiring an energy approximately smaller by 1 eV than the dissociation energy of HX, for the three hydrogen halides. Since the first transition states are much lower than these second ones, it is clear that if energy is provided to the system at the threshold to reach the lowest transition state, then the reaction proceeds always via  $TS$  and leads to the linear HCCX isomer. The triplet states evolve towards the first triplet states of the tetra-atomic systems which are located higher in energy than the singlet.

For the C<sub>2</sub> + H<sub>2</sub> reaction, which is also exothermic ( $\Delta E = 6.36$  eV calculated here with the same ansatz - MRCI +Q/aVQZ) and which requires to break the hydrogen bond ( $D_e = 4.73$  eV)

the activation barrier is only 0.126 eV (exp)<sup>29</sup> and 0.44 eV (MP2 calculation)<sup>13</sup> and the proposed mechanism consists in inserting C<sub>2</sub> into the H<sub>2</sub> bond, eventually via the iso-form. Here, even though the energetic data are very close to those of C<sub>2</sub> + H<sub>2</sub>, it is found that the three halogen systems present larger activation barriers to reach the tetra-atomic systems and that the mechanism proceeds certainly directly to the linear form.

## Conclusions

In this contribution it is shown that the interactions at long and intermediate distances between C<sub>2</sub> and HX can oriente the HX molecule either along the C-C axis, or perpendicular to this axis. For this family of systems, the interaction wells are deeper for HX approaching the  $\pi$  C-C bond perpendicular to its axis, showing the nucleophilic character of C<sub>2</sub> and they increase from HBr to HF due to the larger polarisation of the HF bond than that of HCl and HBr. For the T-shape approach (with HX perpendicular to the C-C axis), the interaction wells are slightly smaller, showing the electrophilic character of C<sub>2</sub> and they increase from HF to HBr due to the larger polarisability and orbital overlapping of HBr than that of HCl and HF. The formation of HCCX or C<sub>2</sub>HX from the two diatomic parts, C<sub>2</sub> and HX, requires an activation energy, smaller than the dissociation energy of HX, ranging from 0.58 eV to 1.70 eV (for HBr to HF) but still large enough to make impossible these exothermic reactions via such a process unless energy is provided to the system. Since the activation energy is smaller for perpendicular approaches, the reaction will finally always lead to the linear HCCX more stable form. As in the molecular tetra-atomic region, the triplet states are always higher in energy than the singlet states in these long range regions and do not contribute directly to the reactivity of these three systems. Another conclusion is that long range interactions of C<sub>2</sub> with polarised molecular systems cannot be treated with mono-reference method due to the particular multi-configurational character of its  $X^1\Sigma_g^+$  ground state.

## References

- (1) Watts, J. D.; Bartlett, R. J. Coupled Cluster Calculations on the  $C_2$  Molecule and the  $C_2^+$  and the  $C_2^-$  Molecular Ions. *J. Chem. Phys.* **1992**, *96*, 6073-6084.
- (2) Watts, J. D.; Bartlett, R. J. Accurate Electron Affinities of Small Carbon Clusters. *J. Chem. Phys.* **1994**, *101*, 409-415.
- (3) Peterson, K. A. Accurate Multireference Configuration Interaction Calculations on the Lowest  $X^1\Sigma^+$  and  $^3\Pi$  Electronic States of  $C_2$ ,  $CN^+$ ,  $BN$  and  $BO^+$ . *J. Chem. Phys.* **1995**, *102*, 262-277.
- (4) Abrams, M. L.; Sherrill, C. D. A Comparison of Polarized Double-zeta Basis Sets and Natural Orbitals for Full Configuration Interaction Benchmarks. *J. Chem. Phys.* **2003**, *118*, 1604-1609.
- (5) Abrams, M. L.; Sherrill, C. D. Full Configuration Interaction Potential Energy Curves for the  $X^1\Sigma_g^+$ ,  $B^1\Delta_g$  and  $B'^1\Sigma_g^+$  States of  $C_2$  : a Challenge for Approximate Methods. *J. Chem. Phys.* **2004**, *121*, 9211-9219.
- (6) Sherrill, C. D.; Piecuch, P. The  $X^1\Sigma_g^+$ ,  $B^1\Delta_g$  and  $B'^1\Sigma_g^+$  States of  $C_2$  : a Comparison of Renormalized Coupled-cluster and Multireference Methods with Full Configuration Interaction Benchmarks. *J. Chem. Phys.* **2005**, *122*, 124104-124110.
- (7) Chaudhuri, R. K.; Freed, K. F. Generation of Potential Energy Curves for the  $X^1\Sigma_g^+$ ,  $B^1\Delta_g$  and  $B'^1\Sigma_g^+$  States of  $C_2$  using the Effective Valence Shell Hamiltonian Method. *J. Chem. Phys.* **2005**, *122*, 154310-154315.
- (8) Purwanto, W.; Zhang, S.; Krakauer, H. Excited State Calculations using Phaseless Auxiliary-field Quantum Monte-Carlo : Potential Energy Curves of Low-lying  $C_2$  Singlet States. *J. Chem. Phys.* **2009**, *130*, 094107-094115.

- (9) Su, P.; Wu, J.; Gu, J.; Wu, W.; Shaik, S.; Hiberty, Ph. C. Bonding Conundrums in the C<sub>2</sub> Molecule : A Valence Bond Study. *J. Chem. Theory Comput.* **2011**, *7*, 121-130.
- (10) Weltner, W.; Van Zee, R. Carbon Molecules, Ions and Clusters. *J. Chem. Rev.* **1989**, *89*, 1713-1747.
- (11) Van Orden, A.; Saykally, R. Small Carbon Clusters : Spectroscopy, Structure and Energetics. *J. Chem. Rev.* **1998**, *98*, 2313-2357.
- (12) Senent, M. L.; Hochlaf, M. Reactivity of Anions in Interstellar Media : Detectability and Applications. *Astrophys. J.* **2013**, *768*, 59-65.
- (13) Skell, P. S.; Jackman, L. M.; Ahmed, S.; McKee, M. L.; Shevlin, P. B. Some Reactions and Properties of Molecular Diatomic Carbon C<sub>2</sub>. An Experimental and Theoretical Treatment. *J. Am. Chem. Soc.* **1989**, *111*, 4422-4429.
- (14) Najar, F.; Ben Abdallah, D.; Jaidane, N.; Ben Lakhdar, Z.; Chambaud, G.; Hochlaf, M. Rotational Excitation and De-excitation of C<sub>2</sub>(X<sup>1</sup>Σ<sub>g</sub><sup>+</sup>) by H<sub>2</sub> (j=0). *J. Chem. Phys.* **2009**, *130*, 204305-204311.
- (15) Lavendy, H.; Robbe, J. M.; Chambaud, G.; Levy, B.; Roueff, E. Theoretical Determination of Intermolecular Potentials of the C<sub>2</sub>-H<sub>2</sub> System. Application to the Collisional De-excitation of C<sub>2</sub> in Collisions with H<sub>2</sub>. *A. and A.* **1991**, *251*, 365-368.
- (16) MOLPRO, version 2012.1, a package of ab initio programs, Werner, H.-J.; Knowles, P. J.; Knizia, G.; Manby, F. R.; Schütz, M. and others, see <http://www.molpro.net>.
- (17) Knizia, G.; Adler, T. B.; Werner, H.-J. Simplified CCSD(T)-F12 Methods : Theory and Benchmarks. *J. Chem. Phys.* **2009**, *130*, 054104-054124.
- (18) Adler, T. B.; Knizia, G.; Werner, H.-J. A simple and Efficient CCSD(T)-F12 Approximation. *J. Chem. Phys.* **2007**, *127*, 221106-221111.

- (19) Boys, S.F.; Bernardi, F. The Calculation of Small Molecular Interactions by the Differences of Separate Total Energies. Some Procedures with Reduced Errors. *Mol. Phys.* **1970**, *19*, 553-566.
- (20) Dunning, T. H., Jr. Gaussian Basis Sets for Use in Correlated Molecular Calculations. The Atoms Boron through Neon and Hydrogen. *J. Chem. Phys.* **1989**, *90*, 1007-1023.
- (21) Ajili, Y.; Hammami, K.; Jaidane, N. E.; Lanza, M.; Kalugina, Y.N.; Lique, F.; Hochlaf, M. On the Accuracy of Explicitly Correlated Methods to Generate Potential Energy Surfaces for Scattering Calculations and Clustering : Application to the HCl-He Complex. *Phys. Chem. Chem. Phys.* **2013**, *15*, 10062-10070.
- (22) Bergner, A.; Dolg, M.; Kuechle, W.; Stoll, H.; Preuss, H. Ab-initio Energy-adjusted Pseudo Potentials for Elements of Groups 13-17. *Mol. Phys.* **1993**, *80*, 1431-1441.
- (23) Martin, J.M.L.; Sundermann, A. Correlation Consistent Valence Basis Sets for Use with Stuttgart-Dresden-Bonn Relativistic Effective Core Potentials : The Atoms Ga-Kr and In-Xe. *J. Chem. Phys.* **2001**, *114*, 3408-3420.
- (24) Huber, K.P.; Herzberg, G. Molecular Spectra and Molecular Structure. Constants of Diatomic Molecules. Van Nostrand Reinhold: New York. **1979**.
- (25) Sileo, R.N.; Cool, T. A. Overtone Emission Spectroscopy of HF and DF : Vibrational Matrix Elements and Dipole. *J. Chem. Phys.* **1976**, *65*, 117-133.
- (26) Piecuch, P.; Spirko, V.; Kondo, A.E.; Paldus, J. Vibrational Dependence of the Dipole Moment and Radiative Transition Probabilities in the  $X^1\Sigma^+$  State of HF: a Linear-response Coupled-cluster Study. *Mol. Phys.* **1998**, *94*, 55-64.
- (27) Kiriya, F.; Rao, B.S. Electric Dipole Moment Function of  $^{79}\text{HBr}$ . *J. Quant. Spectrosc. Radiat. Transf.* **2001**, *69*, 567-572.

- (28) Pecul, M.; Rizzo, A. Relativistic Effects on the Electric Polarisabilities and their Geometric Derivatives for Hydrogen Halides and Dihalogens- a Dirac-Hartree-Fock Study. *Chemical Physics Letters* **2003**, *370*, 578-588.
- (29) Pitts, W. M.; Pasternack, L.; McDonald, J. R. Temperature Dependence of the  $C_2(X^1\Sigma_g^+)$  Reaction with  $H_2$  and  $CH_4$  and  $C_2(X^1\Sigma_g^+$  and  $a^3\Pi_u$  Equilibrated States) with  $O_2$ . *Chem. Phys.* **1982**, *68*, 417-422.

## Figures caption:

Figure 1: Selected geometries of  $[C_2 + HX]$  system.

Figure 2: Cuts of the (MRCI+Q+BSSE) calculated energy functions for the  $[C_2 + HF]$  system in approaches along the C-C axis.

Figure 3: Cuts of the (MRCI+Q+BSSE) calculated energy functions for the  $[C_2 + HF]$  system in approaches perpendicular to the C-C axis.

Figure 4: Cuts of the (MRCI+Q+BSSE) calculated energy functions for the  $[C_2 + HCl]$  system in approaches along the C-C axis.

Figure 5: Cuts of the (MRCI+Q+BSSE) calculated energy functions for the  $[C_2 + HCl]$  system in approaches perpendicular to the C-C axis.

Figure 6: Cuts of the (MRCI+Q+BSSE) calculated energy functions for the  $[C_2 + HBr]$  system in approaches along the C-C axis.

Figure 7: Cuts of the (MRCI+Q+BSSE) calculated energy functions for the  $[C_2 + HBr]$  system in approaches perpendicular to the C-C axis.

Figure 8: Description of the motion of HX around  $C_2$ .

## Tables caption:

Table 1: Energies and structural data of atoms and diatomics of interest calculated at the MRCI level.

Table 2: MRCI structural and energetic data on the  $C_2HX$  and  $HCCX$  isomers.

Table 3: Description of the minima in singlet symmetry for different approaches of  $[C_2 + HX]$  systems calculated at the MRCI+Q+BSSE /aVQZ level.

Table 4: Transition states for Parallel ( $TS$ ) and T-shape ( $TS'$ ) approaches of  $[C_2 + HX]$  systems evaluated at the MRCI level.

**Table 1: Energies and structural data of atoms and diatomics of interest calculated at the MRCI level**

	Method	E (hartree)	$R_e$ (Å)	$\omega_e$ (cm <sup>-1</sup> )	$\mu_e$ (a.u)	$\alpha_{perp}$ (a.u)	$\alpha_{para}$ (a.u)	$\alpha_{iso}$ (a.u)
H( <sup>2</sup> S)	HF	-0.499948						
	HF*	-0.499821						
F( <sup>2</sup> P)	MRCI	-24.142797						
	MRCI*	-24.103709						
Cl( <sup>2</sup> P)	MRCI	-14.891457						
	MRCI*	-14.897488						
Br( <sup>2</sup> P)	MRCI	-13.299601						
	MRCI*	-13.287213						
C <sub>2</sub> (X <sup>1</sup> Σ <sub>g</sub> <sup>+</sup> )	MRCI	-75.795562	1.247	1854.1	0.0	20.40	25.83	22.21
	MRCI*	-75.780784	1.251	1833.9	0.0	21.13	26.02	22.76
C <sub>2</sub> (a <sup>3</sup> Π <sub>u</sub> )	previous		1.242 <sup>b</sup>	1854.71 <sup>b</sup>	0.0	20.5 <sup>a</sup>	25.8 <sup>a</sup>	22.26 <sup>a</sup>
	MRCI	-75.791564	1.317	1632.9	0.0			
HF(X <sup>1</sup> Σ <sup>+</sup> )	MRCI	-24.864362	0.917	4111.2	0.714	4.80	6.10	5.23
	MRCI*	-24.827100	0.917	4134.1	0.706	4.74	6.25	5.24
HCl(X <sup>1</sup> Σ <sup>+</sup> )	previous		0.916 <sup>b</sup>	4138.3 <sup>b</sup>	0.706 <sup>c</sup>			4.92 <sup>f</sup>
	MRCI	-15.560417	1.276	2966.2	0.437	16.34	17.96	16.88
HBr(X <sup>1</sup> Σ <sup>+</sup> )	MRCI*	-15.573386	1.256	3108.0	0.434	15.93	17.46	16.44
	previous		1.274 <sup>b</sup>	2990.9 <sup>b</sup>	0.431 <sup>d</sup>			16.76 <sup>f</sup>
HBr(X <sup>1</sup> Σ <sup>+</sup> )	MRCI	-13.945309	1.415	2623.5	0.321	22.38	24.67	23.14
	MRCI*	-13.928755	1.416	2446.1	0.311	22.70	24.80	23.40
	previous		1.414 <sup>b</sup>	2648.9 <sup>b</sup>	0.322 <sup>e</sup>			23.25 <sup>f</sup>

Values are given for aVQZ basis sets, (\*) are for calculations with aVTZ basis sets.

<sup>a</sup>calculated values from ref. <sup>14</sup>; <sup>b</sup>experimental values from ref. <sup>24</sup>; <sup>c</sup>experimental values from ref. <sup>25</sup>; <sup>d</sup>experimental values from ref. <sup>26</sup>; <sup>e</sup>experimental values from ref. <sup>27</sup>; <sup>f</sup>calculated values from ref. <sup>28</sup>

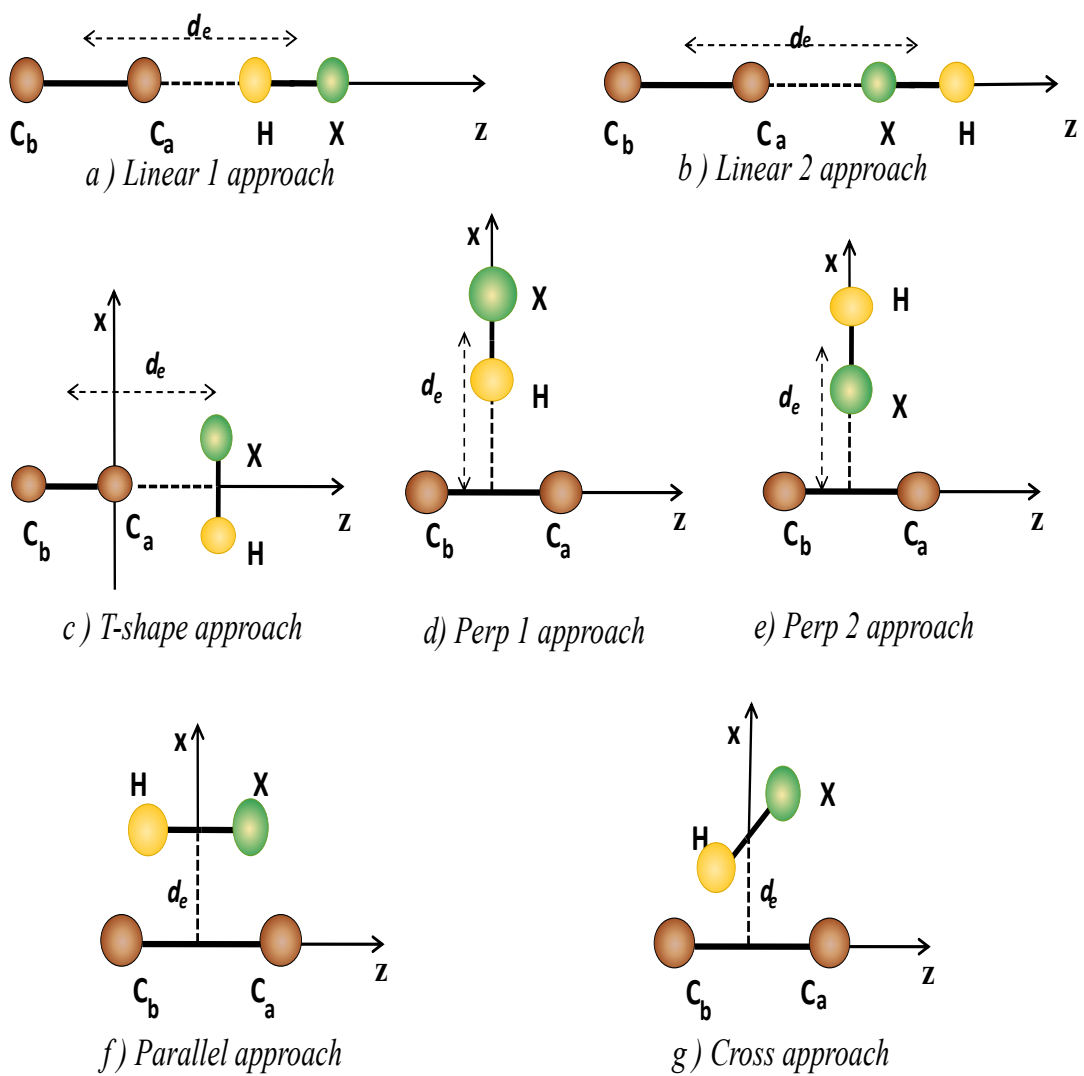


Figure 1: Selected geometries of  $[C_2 + HX]$  system

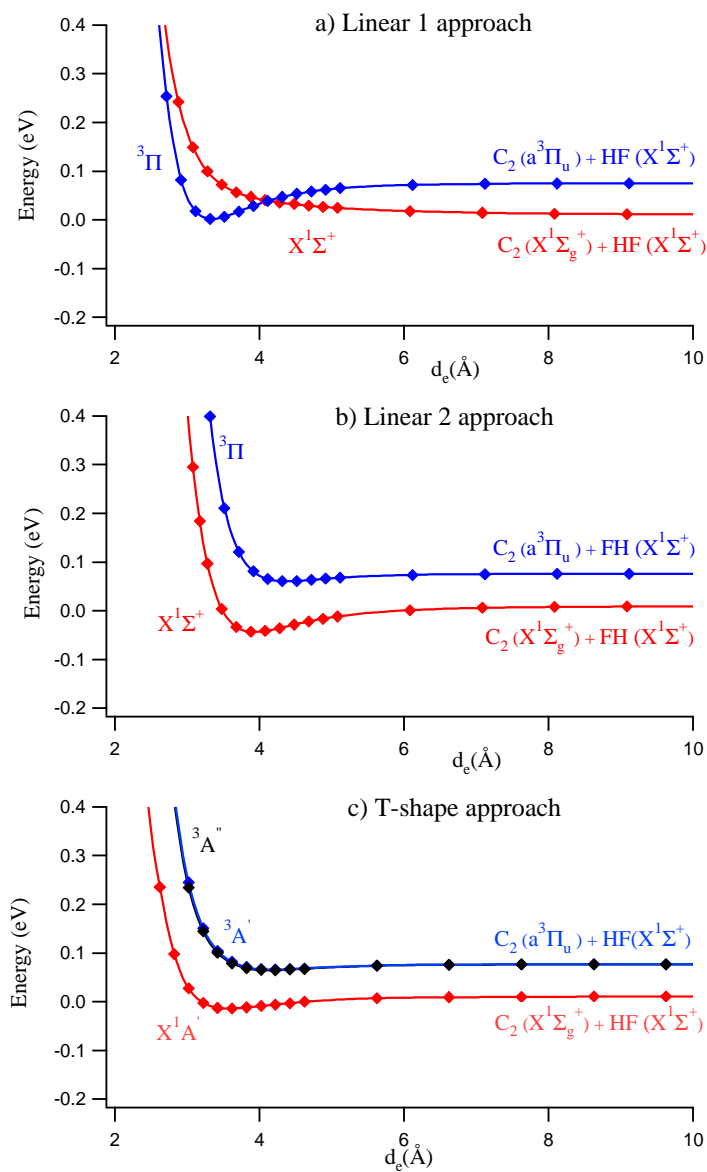


Figure 2: Cuts of the (MRCI+Q+BSSE) calculated energy functions for the  $[C_2 + HF]$  system in approaches along the C-C axis

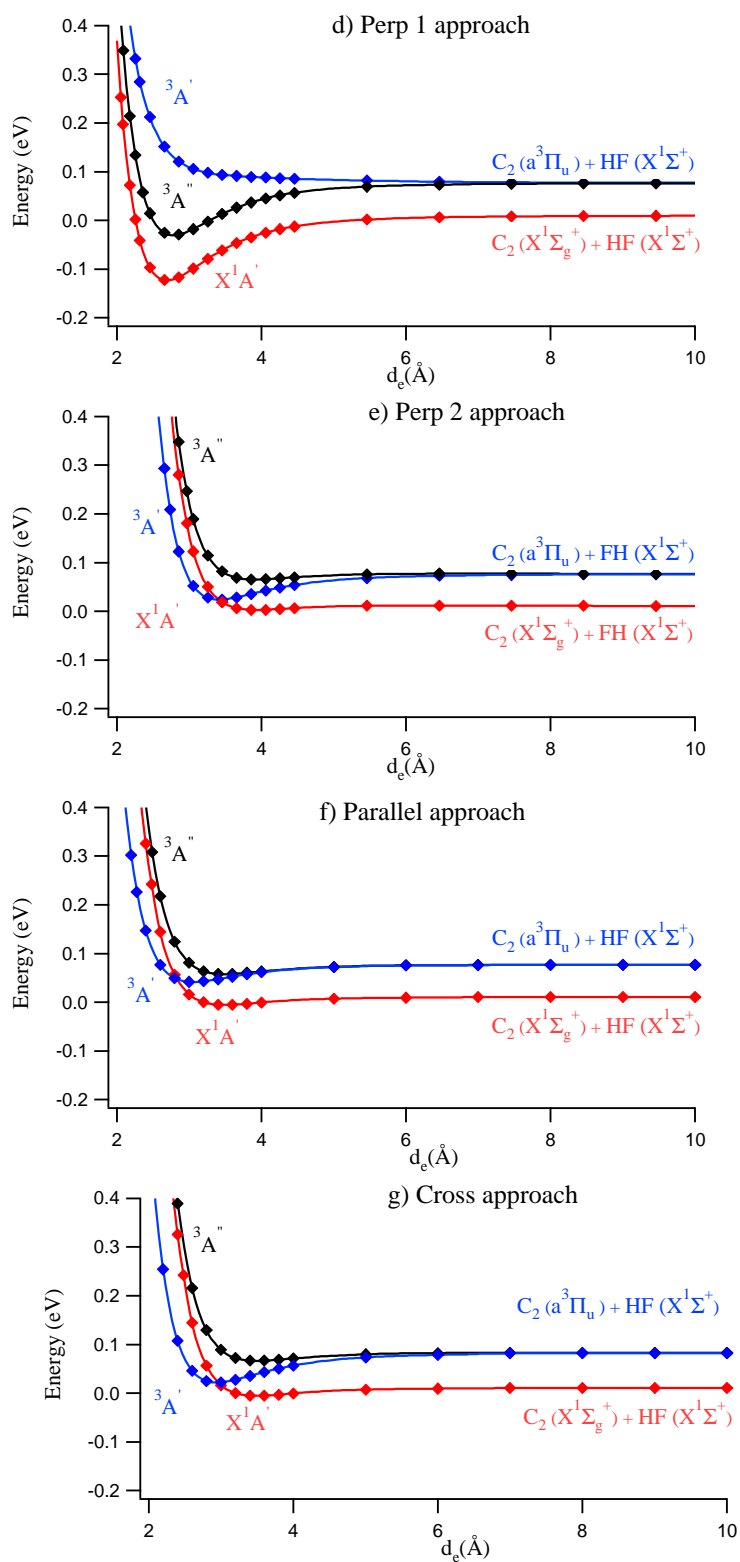


Figure 3: Cuts of the (MRCI+Q+BSSE) calculated energy functions for the  $[C_2 + HF]$  system in approaches perpendicular to the C-C axis

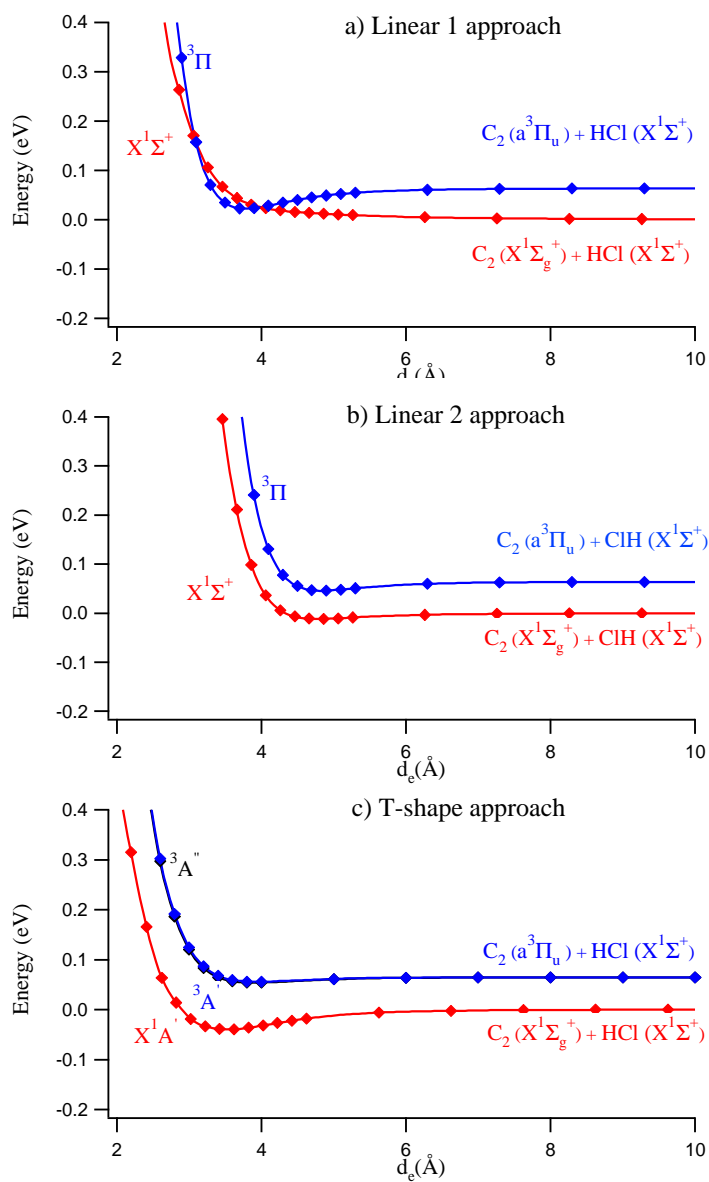


Figure 4: Cuts of the (MRCI+Q+BSSE) calculated energy functions for the  $[C_2 + HCl]$  system in approaches along the C-C axis

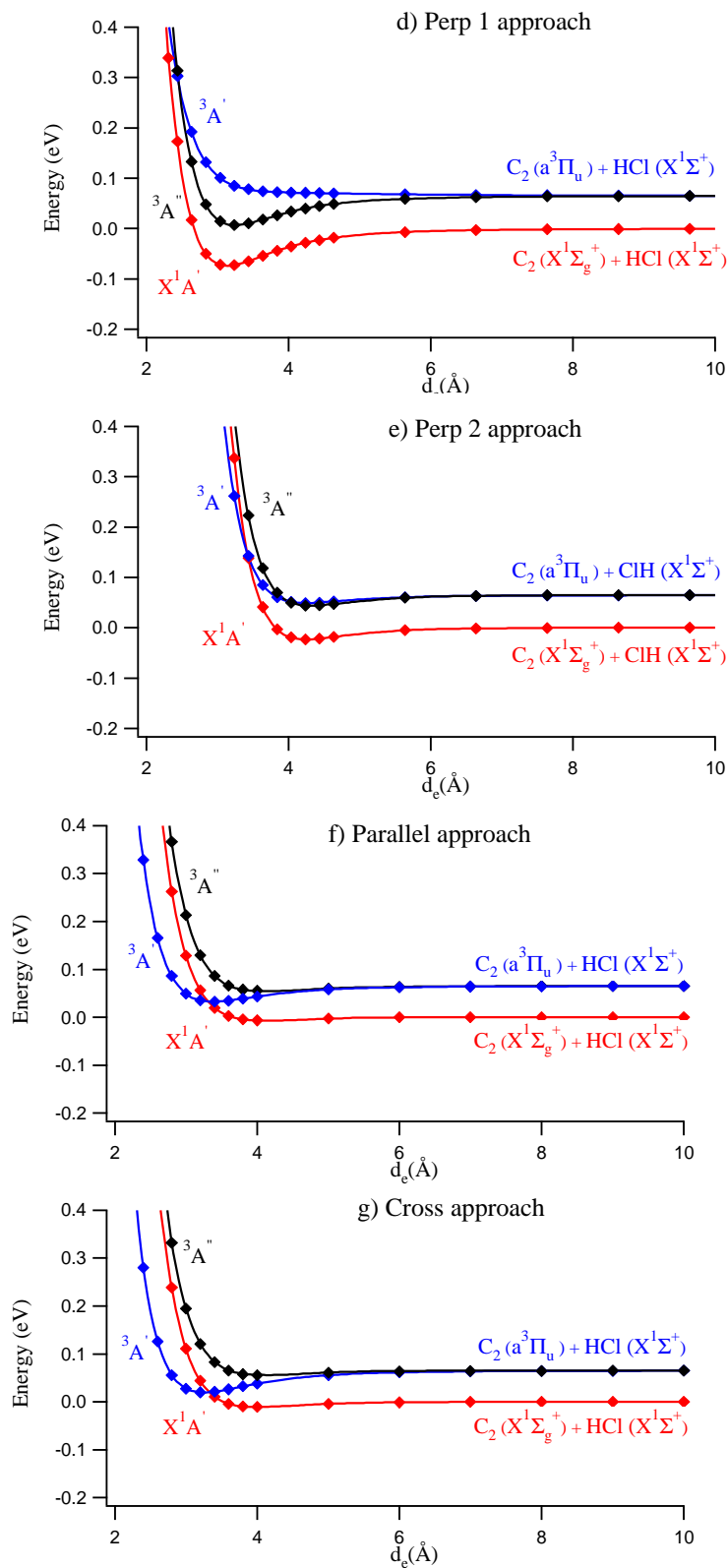


Figure 5: Cuts of the (MRCI+Q+BSSE) calculated energy functions for the  $[C_2 + HCl]$  system in approaches perpendicular to the C-C axis

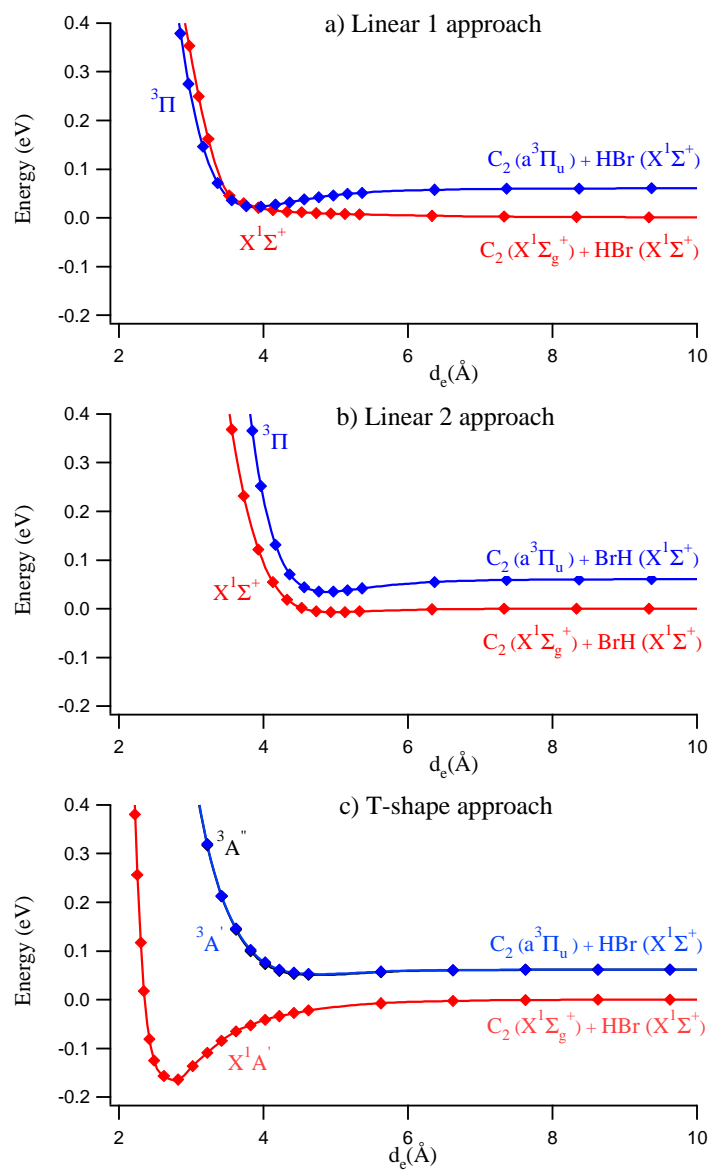


Figure 6: Cuts of the (MRCI+Q+BSSE) calculated energy functions for the  $[C_2 + HBr]$  system in approaches along the C-C axis

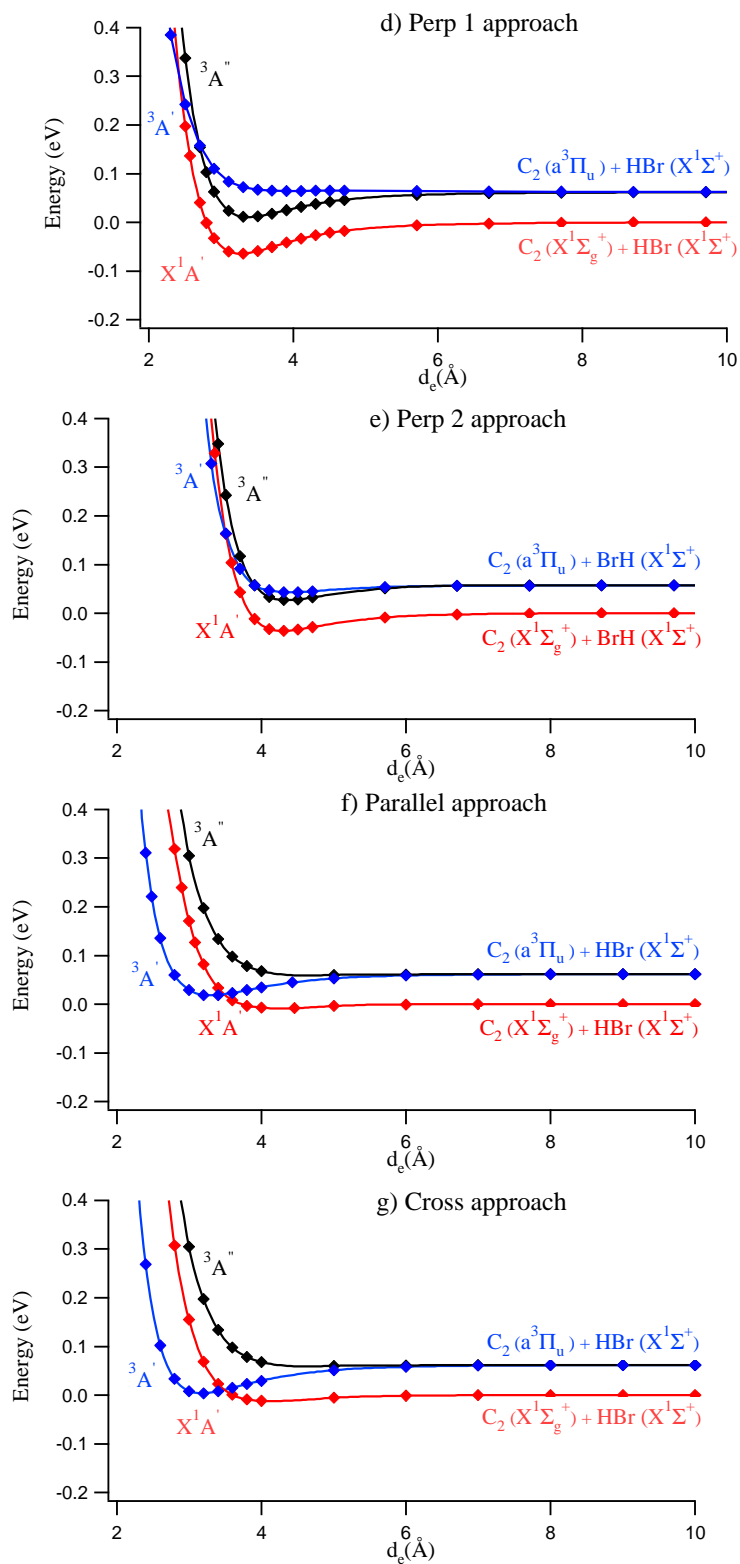


Figure 7: Cuts of the (MRCI+Q+BSSE) calculated energy functions for the  $[C_2 + HBr]$  system in approaches perpendicular to the C-C axis

**Table 2: MRCI structural and energetic data on the C<sub>2</sub>HX and HCCX isomers.**

State	R <sub>C<sub>a</sub>C<sub>b</sub></sub>	Δ E (eV)
C <sub>2</sub> HF( <sup>1</sup> A')	1.328	-2.655
	1.331*	-3.463*
C <sub>2</sub> HCl( <sup>1</sup> A')	1.321	-3.043
	1.320*	-3.063*
C <sub>2</sub> HBr( <sup>1</sup> A')	1.300	-3.216
	1.300*	-3.175*
HC <sub>2</sub> F( <sup>1</sup> Σ <sub>g</sub> <sup>+</sup> )	1.199	-4.714
	1.202*	-5.514*
HC <sub>2</sub> Cl( <sup>1</sup> Σ <sub>g</sub> <sup>+</sup> )	1.206	-5.195
	1.208*	-5.272*
HC <sub>2</sub> Br( <sup>1</sup> Σ <sub>g</sub> <sup>+</sup> )	1.208	-5.253
	1.211*	-5.214*

Δ E (eV) is the energy difference with the associated singlet asymptote [C<sub>2</sub>(X<sup>1</sup>Σ<sub>g</sub><sup>+</sup>) + HX (X<sup>1</sup>Σ<sup>+</sup>)]. Equilibrium distances in (Å), optimised at the MRCI level. Values are given for aVQZ basis sets, (\*) are for calculations with aVTZ basis sets.

**Table 3: Description of the minima in singlet symmetry for different approaches of [C<sub>2</sub> + HX] systems calculated at the MRCI+Q+BSSE /aVQZ level**

Approach	HF		HCl		HBr	
	d <sub>e</sub> (Å)	Δ E (eV)	d <sub>e</sub> (Å)	Δ E (eV)	d <sub>e</sub> (Å)	Δ E (eV)
Perp1	2.71	-0.1344	3.14	-0.0729	3.29	-0.0641
Perp2	3.94	-0.0078	4.27	-0.0229	4.31	-0.0363
Para	3.51	-0.0163	4.26	-0.0075	4.33	-0.0093
Cross	3.54	-0.0124	4.06	-0.0102	4.22	-0.0126
T-shape	3.59	-0.0248	3.56	-0.0395	2.76	-0.1658
Lin2	3.94	-0.0547	4.80	-0.0117	5.00	-0.0071

Δ E (eV) is the energy difference with the corresponding singlet asymptote [C<sub>2</sub>(X<sup>1</sup>Σ<sub>g</sub><sup>+</sup>) + HX (X<sup>1</sup>Σ<sup>+</sup>)]. The calculated absolute energies of [C<sub>2</sub>(X<sup>1</sup>Σ<sub>g</sub><sup>+</sup>) + HX (X<sup>1</sup>Σ<sup>+</sup>)] = -100.67560 hartree ; -91.37150 hartree ; -89.72540 hartree, for X=F, Cl, Br respectively.

**Table 4: Transition states for Parallel ( $TS$ ) and T-shape ( $TS'$ ) approaches of  $[C_2 + HX]$  systems evaluated at the MRCI level**

State	$R_{C_a C_b}$ (Å)	$R_{HX}$ (Å)	$d_e$ (Å)	$\Delta E$ (eV)
$TS_F(^1A')$	1.25	0.93	1.9	1.70
	1.25*	0.96*	1.7*	1.13*
$TS_{Cl}(^1A')$	1.25	1.29	2.3	0.89
	1.25*	1.28*	2.3*	0.84*
$TS_{Br}(^1A')$	1.25	1.43	2.4	0.58
	1.25*	1.43*	2.5*	0.64*
$TS'_F(^1A')$	1.28	2.20	2.65	5.57
	1.28*	2.25*	2.6*	4.57*
$TS'_{Cl}(^1A')$	1.27	2.55	2.7	3.81
	1.27*	2.60*	2.7*	3.97*
$TS'_{Br}(^1A')$	1.26	2.22	2.6	2.13
	1.26*	2.35*	2.5*	1.98*

$\Delta E$  (eV) is the energy of the barrier referred to the corresponding singlet asymptote  $[C_2(X^1\Sigma_g^+) + HX(X^1\Sigma^+)]$ . Values are given for aVQZ basis sets, (\*) are for calculations with aVTZ basis sets.

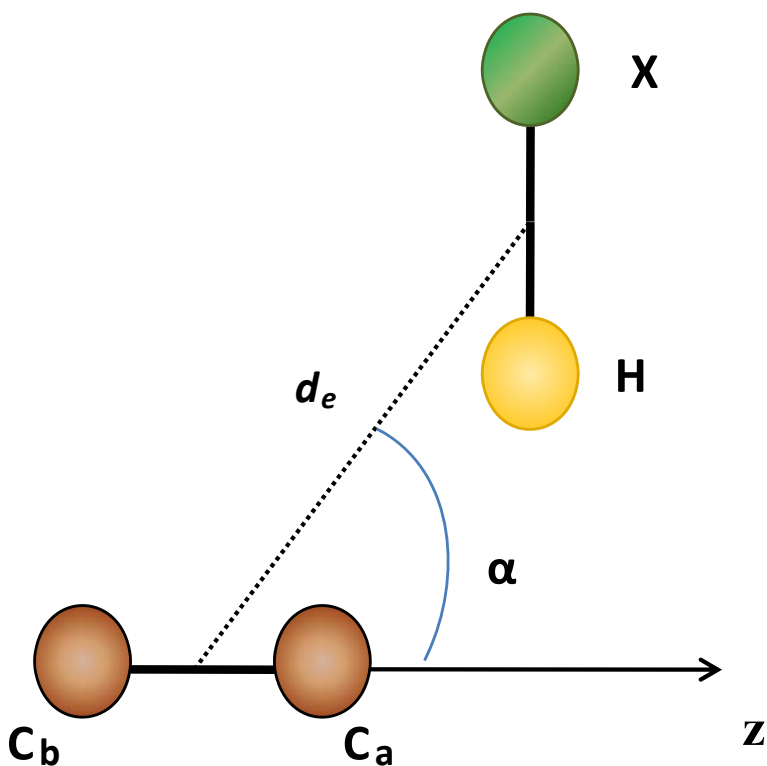


Figure 8: Description of the motion of HX around  $C_2$